Journal of Applied Sciences

ISSN 1812-5654

science alert

ANSInet
an open access publisher
http://ansinet.com

Journal of Applied Sciences 15 (2): 232-239, 2015
ISSN 1812-5654

ansinet
Asian Network for Scientific Information

RESEARCH ARTICLE OPEN ACCESS

DOI: 10.3923/jas.2015.232.239

Investigation of Seismic Footing Settlement Due to Subsidence for the Sand Aquifer with Pumping Wells Using PLAXIS

Su Yang, Amin Chegenizadeh, Mochamad Arief Budihardjo and Hamid Nikraz
Department of Civil Engineering, Curtin University, Perth, Australia

ARTICLE INFO
Article History:
Received: May 27, 2014
Accepted: November 19, 2014

Corresponding Author:
Su Yang,
Department of Civil Engineering,
Curtin University, Perth, Australia

ABSTRACT
Using PLAXIS to evaluate land subsidence due to the extraction of groundwater (i.e., pumping) has long been of interest to researchers. Similarly, the effect of earthquake on land subsidence is an issue worth considering. This study mainly focuses on the effect of groundwater extraction through wells while the site is exposed to seismic forces. The acceleration time series are from two real earthquake cases, one representing small quakes that happen more frequently and the other representing large and extreme quakes. The results showed that a small earthquake with a magnitude of 4.4 has little effect on footing subsidence while a very strong earthquake with a magnitude of 8.8 will increase footing subsidence by one time as compared to the subsidence from a small earthquake. In the meantime, the contribution of the groundwater pumping to the land subsidence is not significant. However, the combination of groundwater pumping and earthquake activity leads to a larger degree of subsidence than other scenarios.

Key words: Footing subsidence, aquifer subsidence, ground water extraction, seismic excitation, PLAXIS modelling

INTRODUCTION

There have been many studies which have discussed footing subsidence problems (Budhu, 2011; Budhu and Adiyaman, 2013; Budihardjo *et al*., 2014a). There have also been a number of incidences of troublesome land subsidence around the world such as Suzhou, China (Shi *et al*., 2012), Aguascalientes Valley, México (Pacheco-Martinez *et al*., 2013) and Hangzhou-Jiaxing-Huzhou, China (Cao *et al*., 2013).

Each of these studies considers an aspect of land subsidence but there has been a lack of research into seismic effects on the whole land subsidence process. Seismic complexity is mainly related to the way that waves are propagated and how they affect the sites and other specific phenomena. The current study aims to add to the body of knowledge on this area by considering the effect of seismic load on land subsidence while wells are extracting groundwater. Previous research at Curtin University has focussed on clay zones and land subsidence (Budihardjo *et al*., 2014a) with an emphasis on footing construction under static loading. This study is part of an integrated parametric study in Curtin University focusing on subsidence and groundwater contamination (Budihardjo *et al*., 2014b). This study will improve upon the previous work by considering seismic effects.

MATERIALS AND METHODS

PLAXIS 2D has an ability to run seismic analysis by incorporating a seismic load to calculate some parameters such as stress, strain and pore pressure. PLAXIS has been equipped with some soil consecutive materials. However, in this study Mohr-Coulomb has been used as a soil material model since it represented a linear elastic plastic material model. The Mohr-Coulomb model also appropriate for 2D plane strain model which was run in this study. The equation of the material model is as follows:

$$\frac{1}{2}(\sigma_1-\sigma_2)+\frac{1}{2}(\sigma_1-\sigma_2)\sin\phi-c\times\cos\phi\le 0$$

The above equation involves the principal stresses in the corresponding plane strain (σ_1 and σ_2), the internal friction angle of the material (ϕ) and also the cohesion of the material

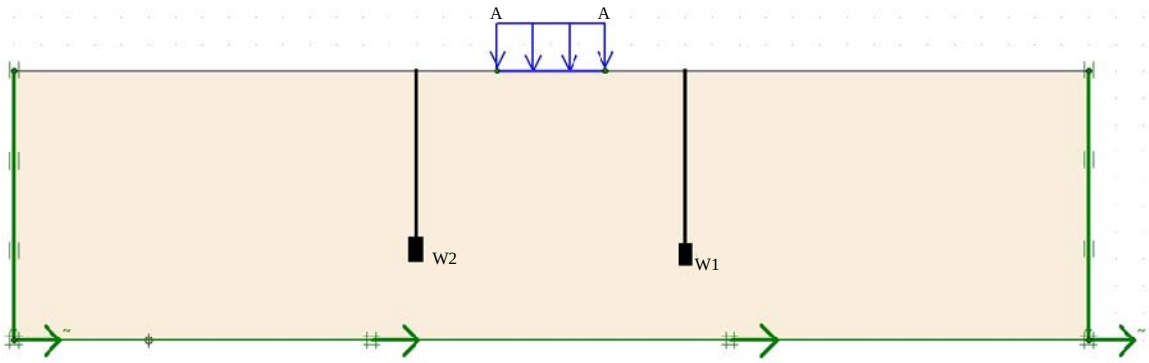

Fig. 1: PLAXIS model of footing on sand aquifer with two pumping wells

(c) (PLAXIS, 2014). Since this model employed a sand which was classified as cohesionless material, formula related to the c value in the equation was ignored. The classical equation also has been followed by PLAXIS to perform dynamic calculations:

$$F = Ma+Ku+Cv$$

The load vector is represented by F, the stiffness matrix is symbolized by K while C and M corresponded to mass matrix and damping matrix, respectively. The acceleration, displacement and velocity are represented by a, u and v. (PLAXIS, 2014).

Another critical factor should be considered when running a seismic modelling is the boundary effect. The use of boundary can trigger the bouncing wave which amplified the seismic energy and provide unreal result of the system. To cope with that problem, viscous boundary was applied to solve the bouncing effect. The viscous boundary has been introduced by Lysmer and Kuhlemeyer (1969) through the following equations:

$$\sigma_n = -C_1\rho V_p v_x$$

$$\tau = -C_2\rho V_s v_y$$

where, the pressure and the shear wave velocity are symbolised by V_P and V_s while the normal and shear stress are represented σ_n and τ. The C_1 and C_2 stand for relaxation coefficient while v_x and v_y represent velocities on relevant directions (PLAXIS, 2014).

Modelling of the problem: PLAXIS was used to model the site, its loads and soil properties. PLAXIS is a finite element method software which is very well-known for soil modelling. The soil properties were entered as input into the model, with the soil being considered as sand with a hydraulic conductivity of 1 m day^{-1}, an initial void ratio of 0.5 and an angle of friction of 32°.

Definition of the geometry in the PLAXIS model: Figure 1 shows the site defined in this study and the elements modelled in PLAXIS. The footing was considered to be a mat foundation with a width of 40 m. The geometry of the soil model was defined as 100×400 m and the model consisted of two wells with an extraction rate of 20 m^3 day^{-1}.

The earthquake records were obtained from two real earthquake recorded by the U.S. Geological Survey, including the magnitude 8.8 earthquake at offshore Maule, Chile (U.S. Geological Survey, 2010) and the magnitude 4.4 earthquake at Encino, California (U.S. Geological Survey, 2014). The larger earthquake in Chile was used to investigate the topic of strong earthquake strikes while the smaller one in California represented small but more frequent quakes (Fig. 2, 3).

RESULTS AND DISCUSSION

Footing settlement due to subsidence after 30 days of pumping: Firstly, footing subsidence caused by water pumping was simulated. The water was pumped for 30 days and the resulting mesh is shown in Fig. 4. The maximum subsidence along the whole surface profile occurred at the centre of the footing which is represented by Node number 1852, with a subsidence of 0.2655 m.

Footing settlement due to subsidence under Encino earthquake: After 30 days' pumping and subsidence with a static distributed load, the earthquake load was applied by inputting an acceleration time series generated by SMC file. According to Fig. 2, significant ground acceleration started at about 32 sec which led into a dynamic duration of 60 sec set for this case calculation. The displacement continued from the previous phase's result (after 30 days of pumping) which is shown in Fig. 4 The resulting deformation mesh after 60 sec of Encino earthquake load is shown in Fig. 5 which is scaled up by 500 times. The vertical displacement at node 1852 is 5.041×10^{-3} m[1]. Compared to 0.2655 m subsidence after pumping, this increase in subsidence is very small and thus

[1]This is the subsidence caused by dynamic phase only, by ticking the box 'reset displacement to zero' in the PLAXIS calculation

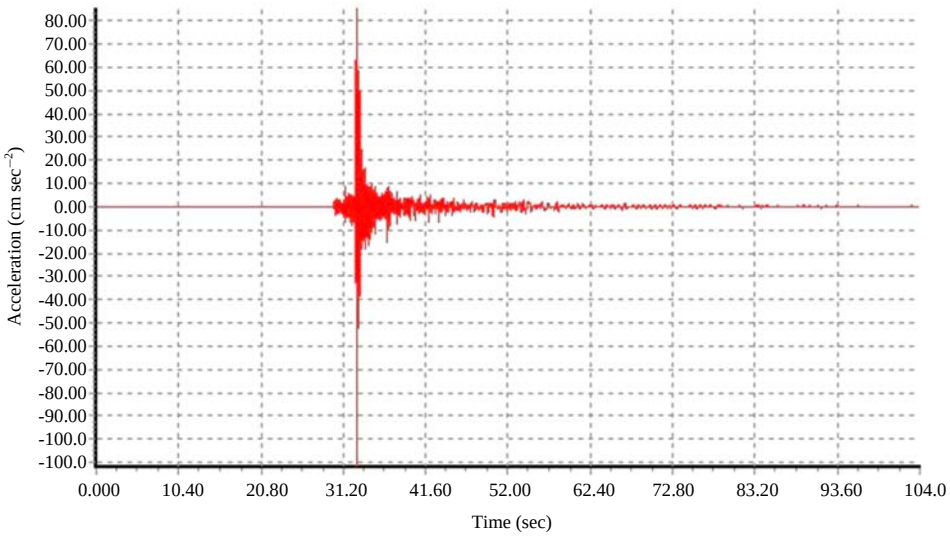

Moment magnitude:	4.40	Epicentral distance:	12.70	km
Surface-wave magniture:	N/A	Peak value:	-112.20	cm sec^{-2}
Local magnitude:	N/A	Sample rate:	200.00	Hz

Fig. 2: Acceleration versus dynamic time diagram for Encino, California earthquake (U.S. Geological Survey, 2014)

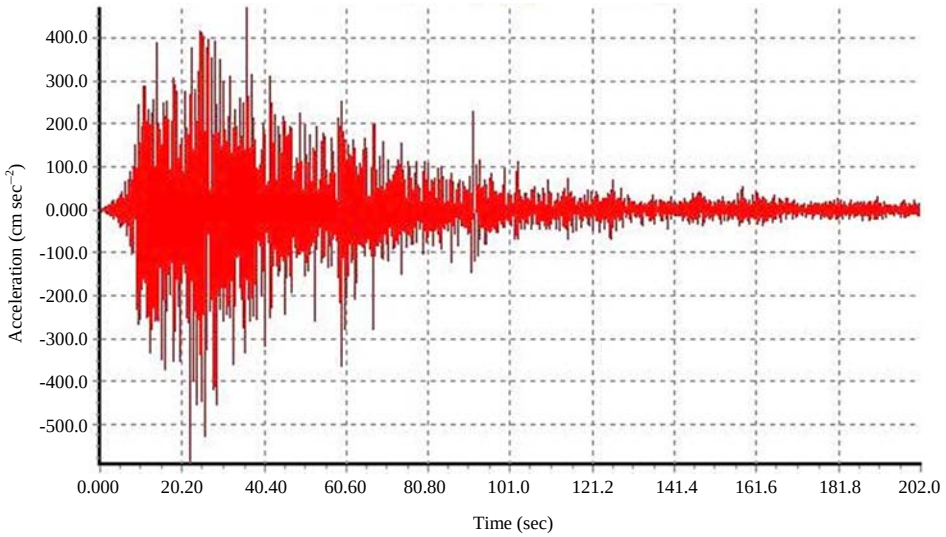

Moment magnitude:	8.80	Epicentral distance:	109.10	km
Surface-wave magniture:	N/A	Peak value:	-594.00	cm sec^{-2}
Local magnitude:	N/A	Sample rate:	100.00	Hz

Fig. 3: Acceleration versus dynamic time diagram for offshore Maule earthquake (U.S. Geological Survey, 2010)

negligible. To sum up the results of this model, there is barely any influence on footing subsidence for earthquakes with small amplitude and a short acceleration period.

Vertical displacement versus dynamic time is plotted in Fig. 6. Almost no subsidence is observed for the first 32 sec, since the small value can be regarded as merely 'computation noise' made by the software in dynamic mode. This corresponds well to the 'peace' period in Fig. 2. The subsidence increased rapidly after the earthquake acceleration began to mount up dramatically (Fig. 2); thus it is safe to deduce that the extra footing subsidence was induced by significant ground acceleration.

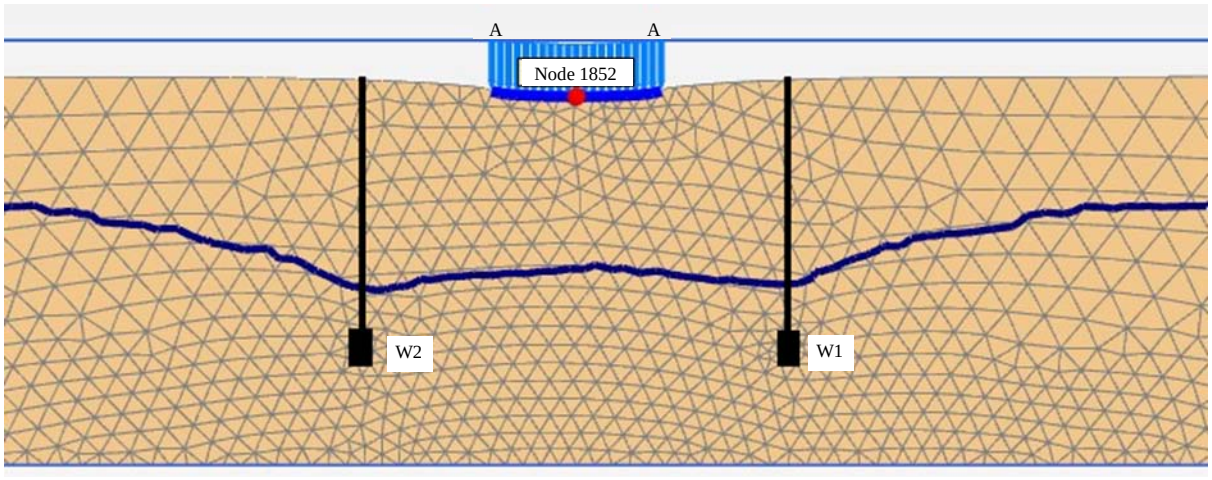

Fig. 4: Deformation mesh after 30 days of water extraction from two wells

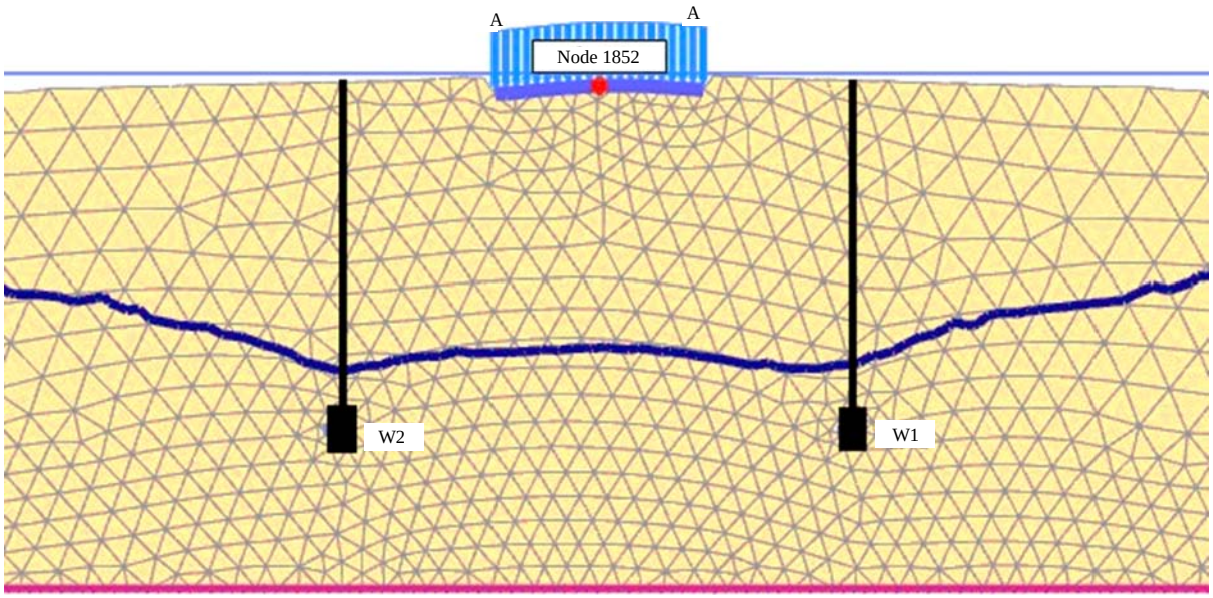

Fig. 5: Deformation mesh after 60 dynamic seconds of the Encino earthquake (500 times scaled up)

Footing settlement due to subsidence under offshore Maule earthquake: This was a strong earthquake lasting for more than 1 min with magnitude of 8.8 (Fig. 3). Similar to the Encino earthquake discussed above, it is following 30 days of water pumping. A dynamic duration of 60 sec was used for the calculation. The resulting deformed mesh is shown in Fig. 7, scaled up by five times. It is necessary to note that the vertical displacement at node 1852 of the footing looks trivial in Fig. 7 but the actual subsidence was 0.241 m, much greater than that for Encino (5.041×10^{-3} m) and this has nearly doubled the subsidence after 30 days of pumping (0.2655 m). The offshore Maule earthquake was much stronger than the Encino earthquake in terms of both acceleration magnitude and period of significant accelerations (Fig. 2 and 3). This indicates a strong earthquake will cause significant footing subsidence.

The vertical displacement versus the dynamic time curve for the offshore Maule earthquake is plotted in Fig. 8. With reference to Fig. 3, there was barely any subsidence for 0-7 sec, after which the subsidence increased dramatically for 1 or 2 sec, then it develops gradually from around 10-30 sec which is also the period of a series of larget accelerations in Fig. 3. There was no further footing subsidence after 20 and 30 sec which corresponded to the period of series of maximum

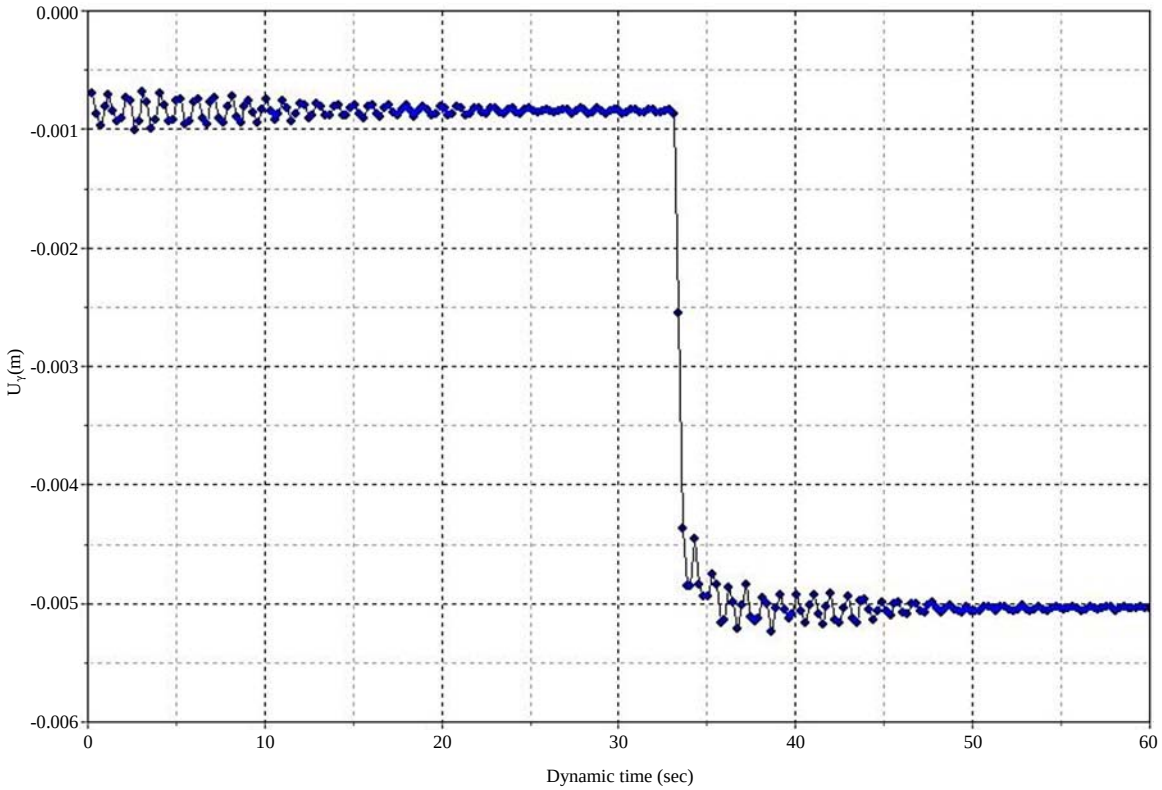

Fig. 6: Vertical displacement with dynamic time curves of node 1852 for the Encino, Carlifornia earthquake

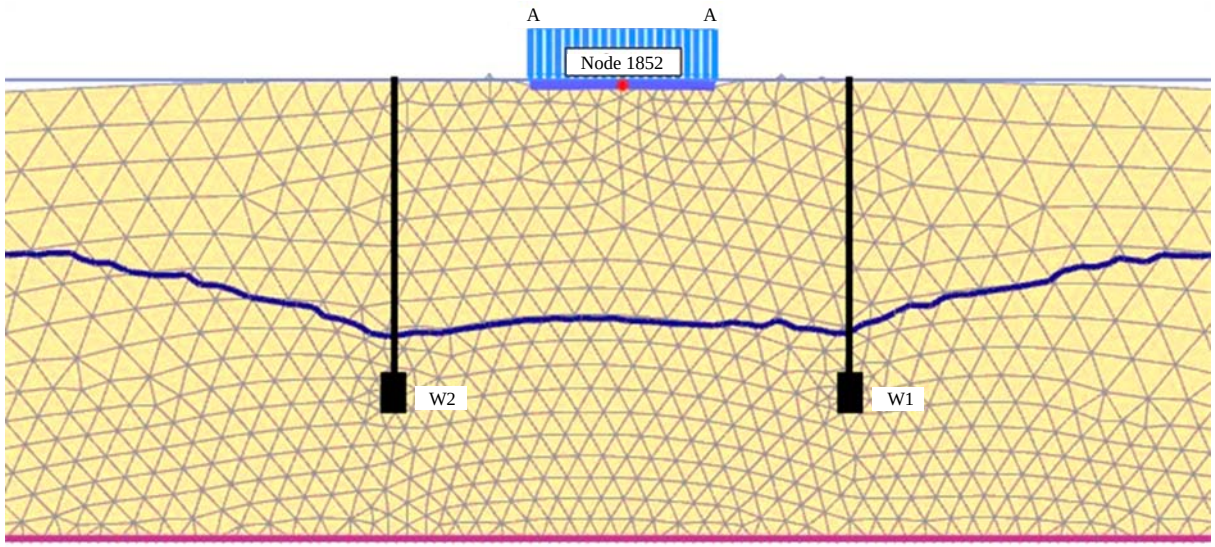

Fig. 7: Deformation mesh after 60 dynamic seconds of the offshore Maule earthquake (five times scaled up)

accelerations in Fig. 3. The subsidence showed little increase after 30 sec, although it has actually continued for 60 sec. It seems therefore that the influence of further, smaller ground accelerations has little influence on footing subsidence, once the maximum acceleration has passed. In other words, the magnitude of seismic footing subsidence is dominated by the largest acceleration level of an earthquake, presumably when the period of this acceleration is sufficient to trigger the corresponding subsidence but this effect is subject to future investigations.

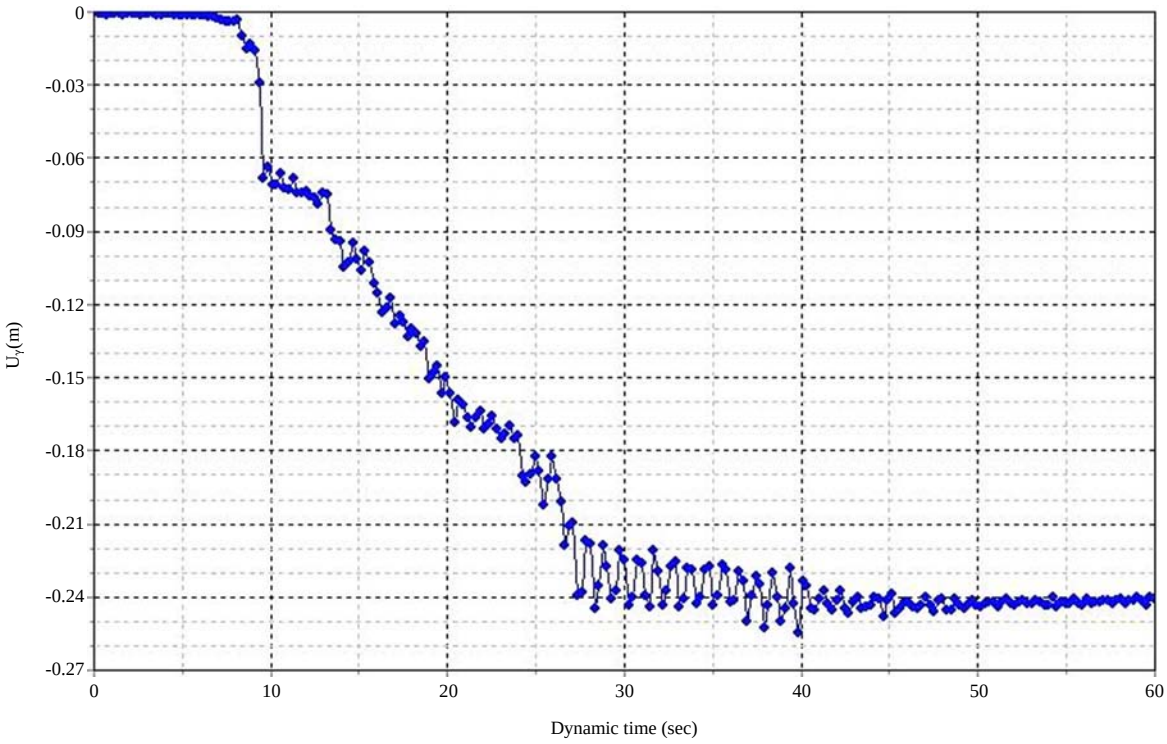

Fig. 8: Vertical displacement with dynamic time curves of node 1852 for the offshore Maule earthquake

Since the maximum acceleration for the Encino earthquake was at a similar magnitude to the acceleration from 0-7 sec of the offshore Maule earthquake, it is reasonable to deduce that there is a threshold acceleration beyond which the subsidence starts to increases significantly.

Footing settlement due to subsidence before pumping: In previous cases, the earthquake load was applied after 30 days of water pumping which lowered the groundwater level significantly as shown in both Fig. 5 and 7. However, earthquake load will change the pore water pressure if water is present and the presence of water will change the behaviour of soil such as reducing the shear strength etc. As a result, in this scenario, the water level is maintained at 10 m below surface.

In this model, the footing was left on the surface for 30 days without pumping and encountered a subsidence of 87 mm, after which the earthquake load of offshore Maule was applied for 60 sec. The deformed mesh after the earthquake is shown in Fig. 9. The node 1852 was subject to an additional 0.340 m of subsidence in Fig. 9. This is around 99 mm more than the 'after pumping' case in Fig. 7. In relation to the displacement versus dynamic time curve, Fig. 10 shows a similar shape to Fig. 8, because they were both under the offshore Maule earthquake influence. However, Fig. 10 demonstrates a greater tendency to subsidence by demonstrating greater final subsidence and a slightly lower initiation time of subsidence, which, as mentioned before, represented the influence cased by series of lower acceleration in Fig. 3. The reason for this phenomenon is probably the weakening of soil strength when the water table is higher, thus more soil material is submerged. A weaker soil then needs smaller acceleration level to trigger dramatic subsidence.

On the other hand, the total subsidence caused by this case (without pumping) is 439 mm while the pumping case is 506.5 mm. Still, water pumping brings about larger overall subsidence.

Comparison with previous studiesand surface subsidence profile: Budihardjo *et al.* (2014a) investigated the influence of water extraction on subsidence of aquifer after 5 years of pumping and it had demonstrated a similar surface profile as indicated in Fig. 4 illustrates the subsidence profile after 30 days of pumping. Thus, both studies indicate that static water extraction has lead into a greatest subsidence at the centre of the aquifer and the subsidence reduces further away from the well location. In contrast to both Fig. 4 and Budihardjo *et al.* (2014a)'s results, this trend is reversed after the seismic excitation of both small and strong earthquakes. As demonstrated in Fig. 5, 7 and 9, the subsidence is lowering towards the centre of the aquifer and increasing further away from the well and footing location. However, the

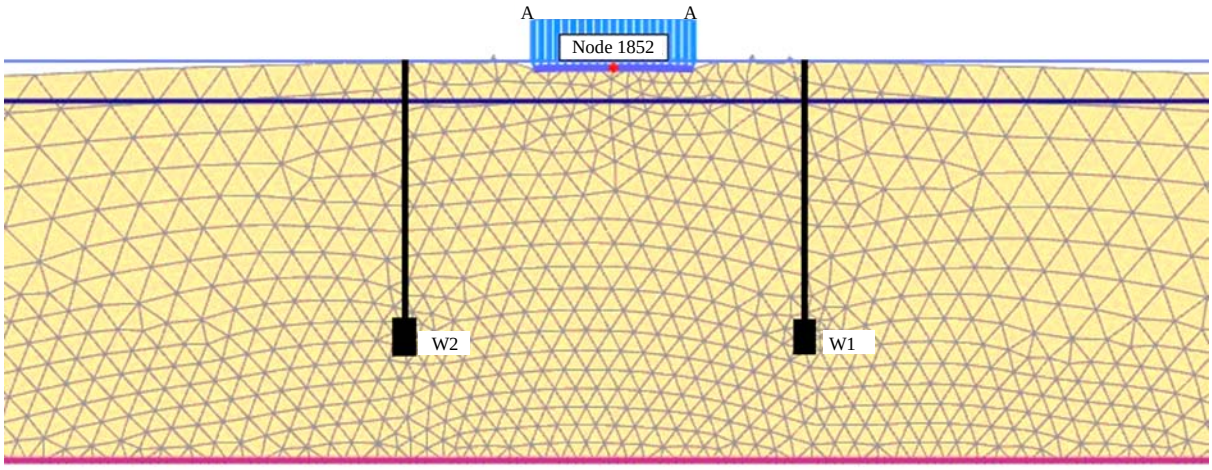

Fig. 9: Deformation mesh after 60 dynamic seconds of offshore Maule earthquake (without 30 days of water pumping)

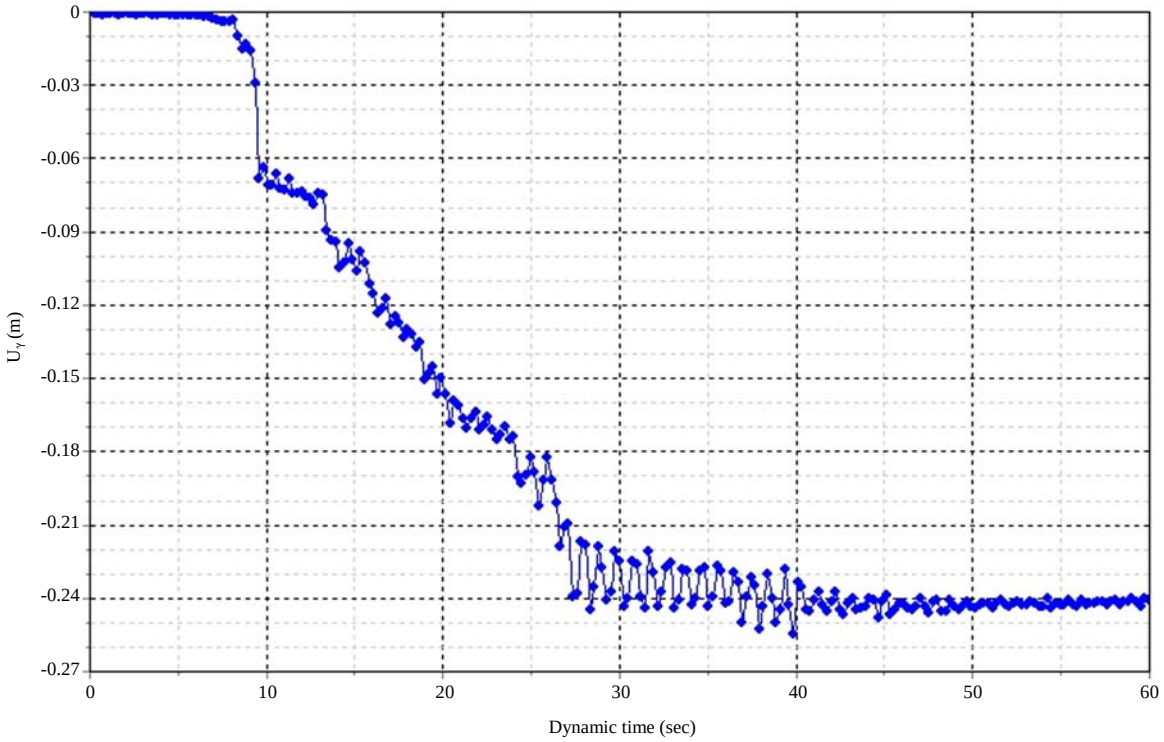

Fig. 10: Vertical displacement with dynamic time curves of node 1852 for offshore Maule earthquake (without water pumping)

subsidence subjects to abrupt increase again when the surface profile reached the footing area (centre of the aquifer) as seen in Fig. 5, 7 and 9. Considering both Budihardjo *et al.* (2014a) and Fig. 2 are for static cases, Fig. 5, 7 and 9 demonstrates that earthquake excitation can lead into a different surface subsidence profile to static water extraction.

CONCLUSION

The effect of seismic on land sibsisdense has been investigated while extracting water from two wells. In order to get better understanding of seismic, two different seismic hsitory data were considered. The seismic data were real and

extracted from U.S. Geological Survey. Subsidence in a sand aquifer with pumping wells was further investigated under earthquake excitation, using two different earthquake records and changing water table conditions. PLAXIS results showed that a small earthquake (such as the earthquake of magnitude of 4.4 investigated in this study) has little effect on footing subsidence. In contrast, a very strong earthquake, like offshore Maule earthquake with a magnitude of 8.8, will significantly further increase footing subsidence (by one time in this case) in a sand aquifer after 30 days of pumping. The degree of extra footing subsidence is dominated by the magnitude of maximum ground acceleration while the acceleration needs to reach a threshold level to cause significant subsidence. Regarding the influence of water pumping, it is concluded that the lowering of the water table induced by water pumping leads to lower subsidence. However, the total subsidence caused by both water pumping and earthquake is still larger than that caused by earthquake alone. In addition, soil shear strength is probably a soil parameter that determines the magnitude of subsidence and the threshold acceleration for 'significant subsidence', that is, a lower strength soil material (e.g., submerged) incurs a larger subsidence and the subsidence starts to increase dramatically at a lower threshold acceleration. With reference to surface subsidence profile, seismic excitation, despite small or strong, produces similar subsidence profiles with the subsidence increasing further away from the well and a dramatic subsidence increase in footing area. This suggests that seismic excitations reversed the trend that is solely caused by extraction of water. However, although an absorbent boundary is used, this simulation prohibits vertical and horizontal movements at boundaries which does not represent either continuous soil ground or more complex geological distribution. Else, using a normal sand model without considering damping and vertical acceleration is away from reality. However, it is still sufficient to give a general idea of how much and when the earthquake horizontal shaking incurs footing subsidence and the influence of the water table on it. In reality, earthquakes may cause liquefaction and highly disturbed ground profiles, so some areas of ground may subside while some others may heave. Future research should address this 'threshold' level for different soil types and ground conditions, since only earthquakes exceed this threshold level, causing problematic subsidence. Also, more earthquake records can be investigated to derive a numerical relationship between acceleration and footing subsidence.

REFERENCES

Budhu, M. and I. Adiyaman, 2013. The Influence of clay zones on land subsidence from groundwater pumping. Groundwater, 51: 51-57.

Budhu, M., 2011. Earth fissure formation from the mechanics of groundwater pumping. Int. J. Geomech., 11: 1-11.

Budihardjo, M.A., A. Chegenizadeh and H. Nikraz, 2014a. Land subsidence: The presence of well and clay layer in aquifer. Aust. J. Basic Applied Sci., 8: 217-224.

Budihardjo, M.A., A. Chegenizadeh and H. Nikraz, 2014b. Prediction of heavy metal contamination from landfill: Lead and chromium. Aust. J. Basic Applied Sci., 8: 207-214.

Cao, G., D. Han and J. Moser, 2013. Groundwater exploitation management under land subsidence constraint: Empirical evidence from the Hangzhou-Jiaxing-Huzhou plain, China. Environ. Manage., 51: 1109-1125.

Lysmer, J. and R.L. Kuhlemeyer, 1969. Finite dynamic model for infinite media. J. Eng. Mech. Div., 95: 859-878.

PLAXIS, 2014. PLAXIS scientific manual. http://www.plaxis.nl/files/files/2DAnniversaryEdition-4-Scientific.pdf

Pacheco-Martinez, J., M. Hernandez-Marin, T.J. Burbey, N. Gonzalez-Cervantes, J.A. Ortiz-Lozano, M.E. Zermeno-De-Leon and A. Solis-Pinto, 2013. Land subsidence and ground failure associated to groundwater exploitation in the aguascalientes valley, Mexico. Eng. Geol., 164: 172-186.

Shi, X., R. Fang, J. Wu, H. Xu, Y.Y. Sun and J. Yu, 2012. Sustainable development and utilization of groundwater resources considering land subsidence in Suzhou, China. Eng. Geol., 124: 77-89.

U.S. Geological Survey, 2010. National strong-motion project earthquake data sets. 20100227 06:34 UTC Mw 8.8 Offshore Maule, Chile Earthquake. http://nsmp.wr.usgs.gov/data_sets/20100227_0634.html

U.S. Geological Survey, 2014. National strong-motion project earthquake data sets. 20140317 13:25 UTC Mw 4.4 Encino, California Earthquake. http://nsmp.wr.usgs.gov/data_sets/20140317_1325.html